PAPER

CrossMark
click for updates

Development of polymerizable 2-(1-naphthyl)-5-phenyloxazole scintillators for ionizing radiation detection†

Ayman F. Seliman,*[a] Valery N. Bliznyuk,[a] Scott M. Husson[b] and Timothy A. DeVol[a]

The synthesis, chemical characterization and optical properties of 2-(1-naphthyl)-4-vinyl-5-phenyloxazole (vNPO) and 2-(1-naphthyl)-4-allyl-5-phenyloxazole (allylNPO) monomers are reported. Starting with the organic fluor 2-(1-naphthyl)-5-phenyloxazole (αNPO), the vNPO and allylNPO monomers were synthesized using Stille coupling followed by purification. The final products were obtained with yields of ~95% and ~55% for vNPO and allylNPO. The absorption/emission spectra of αNPO, vNPO and allylNPO revealed that vNPO has the largest red-shifted in emission with an average wavelength of ~420 nm, which is an advantage for increasing photomultiplier tube sensitivity without the need to add a wavelength shifter. Stable scintillating resin beads were prepared through copolymerization of the newly synthesized fluor monomers with styrene or 4-methylstyrene and divinylbenzene in the presence of toluene porogen. The resin beads were chemically stable and retained the ability to scintillate efficiently after energy deposition of beta particles from ^{99}Tc. This result indicates efficient energy transfer occurs from the base polymer to the covalently attached fluors with subsequent fluorescence in the presence of ionizing radiation.

Introduction

Rapid and sensitive methods for detection of radionuclides in environmental samples are critically important in assuring public health and safety through (1) control and monitoring of air, soil, biosphere, groundwater and surface water contaminated with radioactive materials; (2) monitoring the fate and transport of radionuclides for risk assessment; and (3) detecting the location of clandestine nuclear activities. Thakkar *et al.*[1] developed a new method that combines solid phase extraction and liquid scintillation counting (LSC) in two successive steps to measure total alpha activity in water samples. Although the method demonstrated faster sample preparation, lower detection limits and shorter counting times relative to the traditional method of gas flow proportional counting, it still requires several handling steps and is less selective for detecting specific radionuclides.

Flow analysis is considered an efficient and universal method for radiometric analysis. The essential feature of the flow analysis includes a full automated control over the fluid flow, which enables control of its volumetric flow rates and detection conditions. Such control improves the efficiency of measurements, provides a good reproducibility of results, minimizes personal exposure and maximizes measurement accuracy by mechanization of the performed processes.[2] Furthermore, flow injection methods significantly reduce secondary waste compared to batch analytical procedures. Grate *et al.*[3] first developed a new flow analysis system for determination of ^{90}Sr in nuclear waste through on-line separation and subsequent detection. In the separation step, the Sr-resin was used to eliminate ^{90}Y and other interfering radionuclides. In the detection step, the eluate was mixed with scintillation liquid and transported to the flow-through liquid scintillation counter.

Amongst radiometric flow analysis methods, those that combine the extraction and scintillation processes in a single step have been reported to be rapid and effective for quantification of radioactivity in environmental water samples. DeVol *et al.*[4] and Egorov *et al.*[5] co-immobilized organic scintillating fluors 2,5-diphenyloxazole (PPO) as a primary solute and 1,4-bis(4-methyl-5-phenyloxazol-2-yl) benzene (DM-POPOP) or 1,4-bis(2-methylstyryl) benzene (bis-MSB) as a wavelength shifter with Aliquat-336 extractant within polymer support beads for simultaneous concentration and quantification of ^{99}Tc. The wavelength shifting dye is used in low concentrations (0.01–0.5%) to move the

[a] *Environmental Engineering and Earth Sciences, Clemson University, Anderson, SC 29625, USA. E-mail: ayman@clemson.edu*
[b] *Chemical and Biomolecular Engineering, Clemson University, Clemson, SC 29634, USA*

† Electronic supplementary information (ESI) available: Listing of chemical analysis, scintillation measurement setup, ^{13}C spectra, GCMS chromatograms, optical image for the plastic beads and absorption/emission spectra. See DOI: 10.1039/c5tc00308c

This journal is © The Royal Society of Chemistry 2015

J. Mater. Chem. C, 2015, **3**, 7053–7061 | 7053

emission wavelength to match the spectral sensitivity of PMTs and may also function to reduce the probability of self-absorption of the scintillation light. DeVol *et al.*, reported a minimum detectable concentration lower than required to meet the US Safe Drinking Water Act primary standard.[4]

Radiometric flow analysis using extractive scintillating resins was used successfully to quantify various radionuclides. However, the detection efficiency decreased regularly during subsequent loading and elution cycles, which was attributed to either washing out or to degradation of organic fluors and/or the extractants from the resins. DeVol and his research group reported that the detection efficiency for ^{99}Tc decreased from 50% to 1% by the fifth trial elution using 8 M HNO_3. Two different approaches were tried to overcome or limit the effect of this problem; the first one was achieved by encapsulating the organic fluor within the resin by grafting a thin layer of polymer from the beads surface by atom transfer radical polymerization.[6] Although the sensors prepared with these resins exhibited favorable selectivity and detection efficiency, an approximate 7% decrease in the counting rate was reported as a result of organic fluor leaching after pumping approximately 5000 column void volumes (~1400 column volumes) of 25% (v/v) CH_3OH/H_2O solution. In the second approach, stable scintillating particles were prepared by copolymerization of the 2-[4-(4′-vinylbiphenylyl)]-5-(4-*tert*-butylphenyl)-1,3,4-oxadiazole monomer (vPBD) (was synthesized from the commercial organic flour 2-(4-*tert*-butylphenyl)-5-(4-biphenylyl)-1,3,4 oxadiazole (*t*-butylPBD)) with styrene, divinylbenzene, and 4-chloromethyl styrene mixture.[7] The resin which has been prepared by this method was used effectively to measure $^{99}TcO_4^-$ in several natural freshwater samples with different chemical composition. The emission wavelength of *t*-butylPBD is 365 nm; whereas the optimum wavelength value of most photomultiplier (PMT) is ~420 nm. Thus, to achieve higher detection efficiency *t*-butylPBD should be used with a wavelength shifter. Unfortunately, there is no commercially available monomer form of a suitable secondary fluor, and adding vinyl group to one of the common fluors is problematic for organic synthesis due to the limited solubility in most common organic solvents (DM-POPOP, 0.25–1.2 g L^{-1}; POPOP, 0.05–0.8 g L^{-1}; bis-MSB, 0.1–0.9 g L^{-1}). Needed is an organic fluor monomer that can transfer energy from the base polymer and emit light at the optimum wavelength for the PMT without a wavelength shifter.

Three 1,8-naphthalimide derivatives were synthesized as fluorophore monomers for n/γ discrimination.[8] One of the monomers (4-allyloxy-1,8-naphthalimide) looks promising candidate as a secondary fluorophore ($\lambda_{abs} = 370$; $\lambda_{em} = 430$) especially for PPO. Bagán *et al.*[9] tried another approach through synthesizing microparticles crosslinked plastic scintillator for α and β determination in organic and aggressive media. The material performance was not affected by the characteristics of the measurement solutions. Recently, the vinyl form of PPO was synthesized and characterized for neutron detection. Although, the entire synthesis yield from 6 successive steps was very low (1.7%), the plastic scintillator provided superior n/γ discrimination capabilities and mechanical properties.[10]

PPO is the most commonly used organic fluor for scintillation applications due to its excellent solubility in most solvents, high scintillation efficiency at low concentration and moderate price.[11] However, there is significant loss in light yield at high concentrations[12] and its need for a secondary scintillator or wavelength shifter for proper application are the major shortcomings of PPO. 2-(1-Naphthyl)-5-phenyloxazole (αNPO) is another oxazole material with high quantum yield and large Stokes shift ($\lambda_{abs} = 329$ nm; $\lambda_{em} = 398$ nm) that enables it to measure radioactivity without adding a secondary scintillator. αNPO was applied recently in different radiometric applications; however, the extractive scintillating resins prepared with it suffered from different degrees of instability.[6,13]

The main objective of this work was to prepare stable and efficient extractive scintillating resins by synthesizing polymerizable forms of αNPO and incorporating them covalently into the resin structure. The synthesis and characterization of 2-(1-naphthyl)-4-vinyl-5-phenyloxazole (vNPO) and 2-(1-naphthyl)-4-allyl-5-phenyloxazole (allylNPO) are described. Moreover, the photophysical properties are reported, including scintillation process results from energy deposition of a β emitter as a preliminary proof of the final application.

Experimental

Materials

All chemicals were used as received except monomers, which were dehibited by passing through a column of basic alumina before use. 2-(1-Naphthyl)-5-phenyloxazole (αNPO), hydrobromic acid, 1-methyl-2-pyrrolidinone, and silica-gel were from Alfa Aesar (USA). Tris(dibenzylideneacetone)dipalladium(0) (Pd$_2$(dba)$_3$) and *N*-methyldioctylamine (MDOA) were from Tokyo Chemical Industry Co. (Japan). *N*-Bromosuccinimide (NBS), allyltributyltin, tributyl(vinyl)tin, CDCl$_3$, and methyl acetate were obtained from Acros Organic (USA). Sodium sulfate and ammonium chloride were from J. T. Baker (USA). Ethanol and methanol were purchased from BDH (UK). 4-Methylstyrene monomer, divinylbenzene (DVB), benzoyl peroxide, toluene, poly(vinyl alcohol) (PVA, average M_W 65 000–124 000 Da, degree of hydrolysis 87–89%), tri(2-furyl)phosphine, and 4-chloromethylstyrene (CMS) were from Sigma-Aldrich. Reagent grade NaCl, diethyl ether, dimethylformamide (DMF), chloroform and hexane were from Fisher Scientific. Hydroxypropyl methylcellulose (HPMC) was from Dow Chemical Co. (USA).

Instrumentation

All ^{1}H and ^{13}C NMR spectra were recorded on a JEOL ECX-300 spectrometer operating at 300 MHz for ^{1}H NMR and 75 MHz for ^{13}C NMR at room temperature and in CDCl$_3$ solvent. The chemical shifts (δ) are reported in ppm and were referenced to the residual solvent peak. The coupling constants (J) are quoted in Hz. A Cary 50 Bio UV-Vis spectrophotometer (Varian, Australia Pty Ltd) was used for absorption spectra measurements. All FTIR spectra in this study were collected using a Thermo Nicolet 6700 FTIR spectrometer (Thermo Scientific;

128 scans, 4 cm^{-1} resolution). All the investigated materials were separated using an Agilent 5975T LTM GC/MSD system based on the following GC conditions: analytical column: Agilent J&W DB-5ms Ultra inert LTM, 30 m × 0.25 mm × 0.33 μm; guard column: 0.5 m column with same stationary phases as the analytical column, connected to injector; carrier gas: helium, constant flow rate, 1.0 mL min^{-1}; LTM oven temperature: 160 °C for 4 min then 12 °C min^{-1} to 290 °C for 15 min. Fluorescence was measured using PTI QuantaMaster 60 spectrofluorometer systems (Photon Technology International, Inc) in the range of 300–600 nm. The Raman spectrometer consisted of an Innova 200 argon ion laser (514.5 nm wavelength at ∼1 mW) and a Triplemate 1377 (Spex) spectrograph interfaced to a liquid nitrogen cooled Model LN1152 CCD detector (Princeton Instruments) operating at −120 °C. Radiation detection was performed on a Packard Tri-Carb 2900 liquid scintillation analyzer.

Organic synthesis

The organic syntheses of vNPO and allylNPO were performed using two successive steps. These include bromination of αNPO followed by Stille cross coupling reaction as reported successfully for other materials.[14] Scheme 1 summarizes the organic synthesis routes of the two monomers.

(i) 2-(1-Naphthyl)-4-bromo-5-phenyloxazole (BrNPO). 2-(1-Naphthyl)-5-phenyloxazole (5.0 g, 18.5 mmol) and N-bromo-succinimide (3.93 g, 22.20 mmol) were added to 100 mL chloroform containing a few drops of hydrobromic acid and heated at 65 °C. After 4 h the mixture was cooled to room temperature and filtered using a 0.45 μm Whatman PTFE syringe filter (GE Healthcare Life Science, USA). After drying the solvent, 50 mL of methanol was added and cooled to precipitate the final product (BrNPO) in a pure form, that was filtered, washed and dried at lowered pressure (yield 4.6 g, 70%). ^{1}H NMR (300 MHz, CDCl$_3$) δ 9.32–9.26 (m, 1H), 8.32 (dd, J = 7.4, 1.2 Hz, 1H), 8.13–8.06 (m, 2H), 7.98 (dd, J = 23.0, 8.2 Hz, 2H), 7.71 (ddd, J = 8.5, 6.9, 1.5 Hz, 1H), 7.65–7.50 (m, 4H), 7.49–7.41 (m, 1H). GCMS m/z = 351.1 (M + H$^+$).

(ii) 2-(1-Naphthyl)-4-vinyl-5-phenyloxazole (vNPO). 2-(1-Naphthyl)-4-bromo-5-phenyloxazole (1250 mg, 3.59 mmol), tris(dibenzylideneacetone)dipalladium(0) [120 mg, 131 μmol (5 mol% Pd)], and tri-2-furylphosphine [190 mg, 820 μmol (20 mol% ligand)] were stirred in 1-methyl-2-pyrrolidinone (50 mL) for 15 min. Tributyl(vinyl)tin (1260 μL; 1367 mg, 4.31 mmol) was added, and the resultant mixture was heated to 65 °C and stirred for 48 h, after which time blackening of the mixture had occurred. The reaction mixture was then stirred with 1 M NaOH for 30 min before being filtered through No. 1 Whatman filter paper. The liquid phase was separated and extracted with 5% (v/v) chloroform in diethyl ether (3 × 50 mL). The combined organic extracts were washed with a saturated aqueous solution of ammonium chloride (4 × 25 mL), dried over sodium sulfate, and concentrated under reduced pressure to give a crude yellow solid. Flash chromatography (20% (v/v) chloroform in hexane) gave vNPO as light green crystals (1000 mg, 94.2%). IR, ν_{max} cm^{-1} 3058, 2957, 1625, 1542, 1412; ^{1}H NMR (300 MHz, CDCl$_3$) δ 9.48 (t, J = 11.2 Hz, 1H), 8.33 (td, J = 7.1, 1.2 Hz, 1H), 7.97 (dd, J = 17.4, 7.9 Hz, 2H), 7.83–7.76 (m, 2H), 7.71 (ddd, J = 8.5, 6.8, 1.4 Hz, 1H), 7.65–7.49 (m, 4H), 7.46–7.38 (m, 1H), 7.05 (dd, J = 17.0, 10.8 Hz, 1H), 6.39 (dd, J = 17.0, 1.9 Hz, 1H), 5.55 (dd, J = 10.8, 1.9 Hz, 1H); ^{13}C NMR (76 MHz, CDCl$_3$) δ 160.1, 145.9, 135.3, 134.1, 131.5, 130.4, 129.1, 128.8, 128.7, 128.6, 128.1, 127.7, 126.6, 126.5, 126.4, 125.9, 125.1, 123.8, 117.7. GCMS m/z = 297.1 (M + H$^+$).

(iii) 2-(1-Naphthyl)-4-allyl-5-phenyloxazole (allylNPO). 2-(1-Naphthyl)-4-bromo-5-phenyloxazole (625 mg, 1.8 mmol), tris(dibenzylideneacetone)dipalladium(0) [60 mg, 65 μmol (5 mol% Pd)], and tri-2-furylphosphine [95 mg, 410 μmol (20 mol% ligand)] were stirred in 1-methyl-2-pyrrolidinone (30 mL) for 15 min. Allyltributyltin (670 μL, 727 mg, 2.29 mmol) was added, and the resultant mixture was heated to 65 °C and stirred for 48 h. Using a modified extraction and purification procedure described for vNPO preparation, flash chromatography (20% (v/v) chloroform in hexanes) gave allylNPO as a light yellow oil, which crystallized in a water/acetonitrile (20 : 80 v/v) solution after cooling at −20 °C giving a light yellow solid (305 mg, 55.0%). IR, ν_{max} cm^{-1} 3058, 3002, 2918,
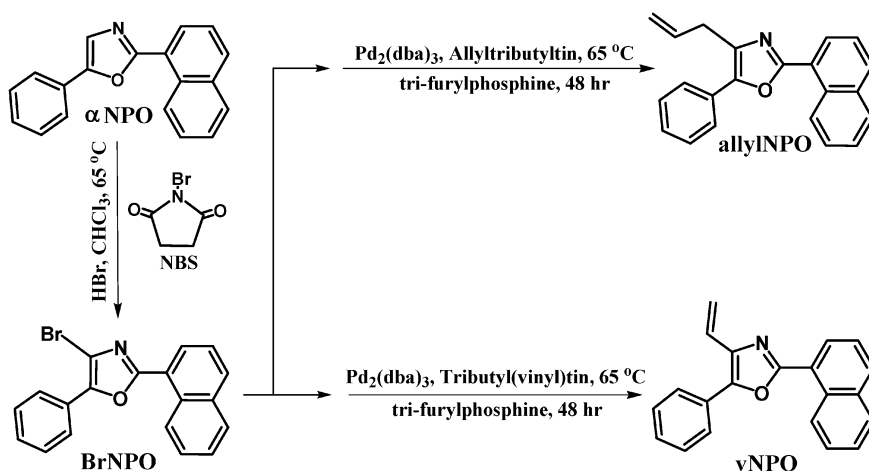
Scheme 1 Synthesis of monomer 2-(1-naphthyl)-4-vinyl-5-phenyloxazole (vNPO) and 2-(1-naphthyl)-4-allyl-5-phenyloxazole (allylNPO).

1639, 1528, 1429; ^{1}H NMR (300 MHz, CDCl$_3$) δ 9.33 (dd, J = 15.3, 8.5 Hz, 1H), 8.32 (ddd, J = 7.3, 4.0, 1.3 Hz, 1H), 8.16–8.07 (m, 1H), 8.06–7.89 (m, 2H), 7.85–7.73 (m, 1H), 7.73–7.65 (m, 1H), 7.65–7.35 (m, 5H), 6.38–6.09 (m, 1H), 5.37–5.08 (m, 2H), 3.73 (dt, J = 5.9, 1.7 Hz, 2H); ^{13}C NMR (76 MHz, CDCl$_3$) δ 159.9, 146.0, 135.3, 134.8, 134.1, 131.2, 130.3, 129.0, 128.7, 128.1, 127.9, 127.7, 126.4, 125.8, 125.1, 124.1, 116.7, 31.9. GCMS m/z = 311.2 (M + H^{+}).

Resin preparation, functionalization and stability

Scintillating polymer resins were prepared as *ca.* 100–400 µm diameter spherical beads *via* suspension polymerization technique. The mixture of styrene or 4-methylstyrene monomer with 4-chloromethyl styrene (CMS), DVB (crosslinker), benzoyl peroxide (initiator) and a toluene porogen was used as a dispersed oil phase. The ratio of the components was varied to adjust the porosity, optical transparency and size of the final polymer beads. The dispersed phase contained also 0.5, 1, or 3.0% (w/w) of organic fluors: αNPO, vNPO or allylNPO. A continuous aqueous phase contained PVA, NaCl and HPMC as emulsion stabilizers. Details of the suspension polymerization method were reported in one of our recent publications.[15] After polymerization, the chlorobenzyl groups from CMS were aminated by reaction with MDOA, which showed high selectivity for pertechnetate anion ([99]TcO$_4$[−]) as a beta emitter radionuclide.[7] A suspension of 1 g resin, 20 mL of DMF and 1 mL of the amine was heated (65 °C) and stirred for 4 h. The beads were washed with 1 M HCl and then water until the wash solution became neutral. They were washed finally with ethanol and left to dry in air. The result was a chemically stable scintillating resin, with covalently bound organic fluor and extractive ligand. The efficiencies of incorporation of the fluorescent monomers into the polymer beads were estimated using three different steps. (1) To washout all un-polymerized fractions, 1 g each of the three polymers (P-αNPO, P-vNPO and P-allylNPO) was mixed with 15 mL of an organic solvent (methyl acetate) and left overnight on an end-over-end stirrer, the resin was filtered and further washed with fresh solvent to remove any surface impurities; organic leachates were tested using UV-Vis absorbance. (2) Elemental analysis (CHN) was conducted for the same beads to measure the total nitrogen of the oxazole group (Elemental Analysis Inc, KY). (3) The scintillation efficiencies of the unwashed and washed samples were measured using about 25 mg of the scintillating beads in 7 mL LSC vial. 1 µCi [241]Am point source was positioned at about 0.5 cm above the bead surface and the light output from α particles deposition was measured using a Hidex Triathler LSC (Fig. S1, ESI†).

Fluorescence and scintillation measurements

Fluorescence properties of organic fluors in solvent and polymer matrices were studied using a double-monochromator spectro-fluorometer system to eliminate background signal and minimize noise due to stray light. To study fluor solutions, a 3 mL square cross-section quartz cuvette was used to hold a solution with a typical fluor concentration of 1 mg mL^{-1} in methyl acetate. To study polymer resin samples, a monolayer of resin beads was attached to 1 cm × 5 cm glass slides using a double-sided

adhesive tape and then placed in the same quartz cuvette in a vertical position with the cuvette cross-section at 45° angles both to the incident light beam and to the PMT slit directions. The molar extinction coefficient of αNPO, vNPO and allylNPO in methyl acetate at 335 nm was measured using UV-Vis, while the corresponding fluorescence quantum yield was calculated using αNPO as a reference material in accordance to a procedure described in ESI.†

Luminosity and scintillation measurements were conducted with the beads in a mini-column sensor geometry using off-line detection. The aminated scintillating resin was dry packed into an FEP Teflon column with a glass frit filter packed at each end to prevent resin washout from the tubing. After passing 0.01 M HCl aqueous solutions containing different concentrations of ^{99}Tc, the whole column was fixed in the center of a 20 mL liquid scintillation glass vial and counted on the LSC as a solid scintillator (Fig. S1, ESI†). A calibration curve was prepared after successive loading of five different ^{99}Tc concentrations. The aim of this experiment was to characterize the scintillation properties, and demonstrate the linearity of the new material for radiation detection and quantification.

Results and discussion

Monomers synthesis and polymer stability

The vNPO and allylNPO monomers were synthesized *via* Stille coupling of tributyl(vinyl)tin and allyltributyltin, respectively, with the electrophile BrNPO. Fig. 1 shows typical ^{1}H NMR spectra of αNPO, vNPO and allylNPO in CDCl$_3$ with signal assignment. The figure confirms the successful organic synthesis of vNPO and allylNPO relative to the starting material (αNPO). Comparing the ^{1}H NMR spectra of αNPO, vNPO and allylNPO, the peak corresponding to the proton of the oxazole group in position 4 (d, 7.62) disappeared after bromination and Stille coupling reactions. The ^{1}H NMR spectrum of the vNPO showed new three peaks: two peaks at 5.54 and 6.38 ppm assigned to the chemical shift of hydrogen in –CH$_2$ of the vinyl group and one peak at 7.04 ppm assigned to the –CH proton of the same vinyl group. The ^{1}H NMR spectrum of the allylNPO showed also three new peaks assigned to five new protons of the allyl group; two protons at 3.72 ppm, two protons at 5.24–5.32 ppm and one proton at 6.20 ppm. The integration of new peaks relative to the area of one stable proton revealed that the chemical conversions of vNPO and allylNPO are 100% and 96%, respectively.

^{13}C NMR was utilized to study the structure of vNPO and allylNPO monomers, and CDCl$_3$ was used as the chemical shift reference, which gives a strong signal at 77.2 ppm. ^{13}C NMR experimental spectra are given in ESI† (Fig. S2). The data analysis reveals that for both materials, oxazole carbons appear as three peaks around 135, 146 and 160 ppm, while the aromatic carbons of phenyl and naphthyl groups appear as multiple signals between 124 and 136 ppm. The vNPO spectrum shows two new peaks at 125.1 and 117.7 ppm assigned to the attached vinyl group and corresponding to C-22 and C-23, respectively. For allylNPO, three new peaks appear in the spectrum, which indicates that the allyl group was added
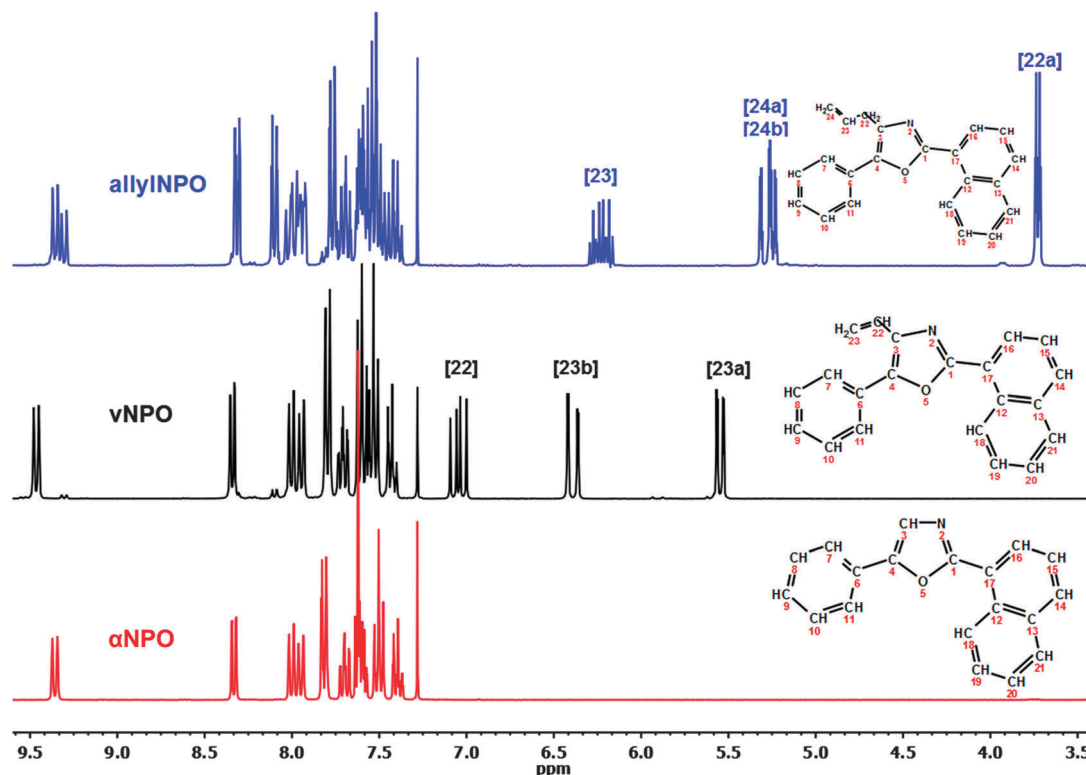
7056 | *J. Mater. Chem. C,* 2015, **3**, 7053–7061

This journal is © The Royal Society of Chemistry 2015

Fig. 1 The NMR spectra for αNPO fluor, vNPO and allylNPO monomers. Cxx refers to the carbon atom on the molecule.

successfully. These peaks include 31.9 ppm for C-22, 116.7 ppm for C-24 and 134.1 ppm for C-23.

A modified GCMS method for quantification of αNPO and its three different derivatives was developed and applied successfully to adjust and track the organic synthesis and conversion of vNPO and allylNPO monomers. Fig. S3 (ESI†) shows the chromatograms of individual and simultaneous separation of the four NPO materials according to the mass order where the starting material αNPO (m/z = 271.1) eluted first at 15.9 min, and the final products vNPO (m/z = 297.1) and allylNPO (m/z = 311.2) eluted at 16.1 and 16.2 min. Finally, the intermediate material BrNPO (m/z = 351.1) eluted at 17.0 min. The GCMS analysis showed that performing organic synthesis reactions in a N_2 atmosphere and allowing 48 h are essential to get the final product in a high yield and with high chemical purity. After establishing good synthetic routes for vNPO and allylNPO monomers, they were incorporated covalently in the resin polymer matrix. Accordingly, vNPO monomer was co-polymerized with styrene or 4-methylstyrene and a cross-linker, DVB using standard suspension polymerization. This procedure was carried out in the presence of toluene, which served as a porogen, and water containing PVA, which acted as a droplet stabilizer. The 10% cross-linked, scintillating macro-porous polymeric beads that resulted from the suspension polymerization process were collected by filtration, washed extensively with methanol, dried in vacuum and then sieved to provide polymer beads with relatively narrow diameter ranges of 100–200 μm or 220–400 μm. Polymer resins containing unbound αNPO fluor were prepared via mixing fluor molecules with the

monomers before the suspension polymerization process. The beads of the same size range (typically, 100–200 μm) were then used for further characterization and comparison. The optical microscopy images show that the scintillating beads are spherical and transparent (Fig. S4, ESI†).

The αNPO and its derivatives have very strong absorption bands from 300–350 nm due to the π–π* conjugate transition in the aromatic structure. These absorption bands were used to investigate the chemical stability of covalently incorporated vNPO and allylNPO monomers. The UV-Vis absorption spectra of the methyl acetate leachates following 24 h batch contact showed negligible amounts of vNPO from P-vNPO, more significant amounts from allylNPO from P-allylNPO (attributed to unreacted fluor monomers) but a high concentration of αNPO from P-αNPO. This result indicates clearly that the scintillating resins are more stable relative to resin with unbound fluor. The elemental analysis further confirmed that, the final mass incorporated in the matrix is 2.85% (w/w) and 1.05% (w/w) for vNPO and allylNPO relative to the starting concentrations of 3% (w/w), while the αNPO washed out completely from P-αNPO. Luminosity measurements of polymer beads before and after washing with methyl acetate using an [241]Am point source revealed that the unwashed P-vNPO, the washed P-vNPO (P-vNPO-L) and the aminated P-vNPO with N-methyl-dioctylamine (P-vNPO-MDOA) have almost the same peak height, which confirms their good stability; whereas the same investigation for the corresponding allylNPO materials revealed that the washed P-allylNPO (P-allylNPO-L) and the aminated P-allylNPO (P-allylNPO-MDOA) have lower peak heights relative

This journal is © The Royal Society of Chemistry 2015

J. Mater. Chem. C, 2015, **3**, 7053–7061 | **7057**

to that of the unwashed P-allylNPO (P-allylNPO) (Fig. S5, ESI†). For P-αNPO resin, the peak height decreased significantly from 500 channels for the resin before washing to <250 channels for the resin after washing, which further supports that the resin with unbound fluor is unstable and cannot be used for radiation detection using an extractive scintillating approach.

FTIR and Raman characterization

The chemical structures of αNPO fluor and vNPO and allylNPO monomers were characterized using FTIR and Raman spectroscopies. Fig. 2 and 3 show the IR and Raman analyses of the three materials. Comparing the IR vibrational spectra reveals a general similarity over the energy range of 700–3300 cm^{-1}. Strong absorption peaks are observed at 1525 cm^{-1} for αNPO and 1528 cm^{-1} for allylNPO, which are shifted to 1542 cm^{-1} in vNPO. These peaks are assigned to C=N stretching in the oxazole group. There are two new peaks at 1625 cm^{-1} and 1639 cm^{-1} for vNPO and allylNPO, respectively, which are assigned to the C=C

Fig. 2 The FTIR spectra of αNPO fluor, vNPO and allylNPO monomers.

Fig. 3 The Raman spectra of αNPO fluor, vNPO and allylNPO monomers.

stretching of vinyl and allyl groups. The same C=C peak was reported by Gauthier et al.[16] at 1640 cm^{-1} for the vinyl group of dimethylacrylate dental monomers. Two new weak peaks are attributed to the C–H bonds of the vinyl and allyl groups of vNPO (1412 cm^{-1}) and allylNPO (1429 cm^{-1}) monomers. The strong peak at 3120 cm^{-1} assigned to C–H group in the oxazole ring at position C4 disappeared in the vibrational spectra of vNPO and allylNPO. This indicates that the vinyl and allyl groups were successfully introduced into the αNPO molecule.

Fig. 3 shows Raman spectra of αNPO fluor, vNPO and allylNPO monomers excited with 514.5 nm emission from an Ar laser. There are two new noticeable peaks at 1632 cm^{-1} for vNPO and 1596 cm^{-1} for allylNPO assigned to the C=C stretching of vinyl and allyl group. Similar peaks were reported at 1639 cm^{-1} and 1662 cm^{-1} attributed to the C=C stretching of fundamental and vinyl isomers of crotyl chloride, respectively.[17] Although the Raman spectra of vNPO and allylNPO are almost identical, the lower energy shift of allylNPO may be attributed to the mass difference of the two monomers, which is affecting the C=C vibration mode frequency.

Absorption and fluorescence properties

Fig. 4 shows the normalized linear absorption and fluorescence spectra for NPO compounds in methyl acetate solution. Absorption bands with primary maxima at 334 for αNPO fluor and 336 nm for vNPO and allylNPO monomers were found, that are attributed to transition of the conjugated aromatic groups. vNPO also shows a strong absorption peak at 296 nm with a higher absorption band between 300 and 350 nm relative to the other two materials. All compounds produced significant fluorescence and emit light of a violet color (Fig. 4).

The fluorescence maxima are located at 398 nm for αNPO and two bands centered at 409 nm and 418 nm for vNPO and allylNPO, respectively. Emission maxima shifted towards longer wavelengths after attaching both vinyl and allyl groups, with a slightly larger shift for vNPO. In previous research Seliman
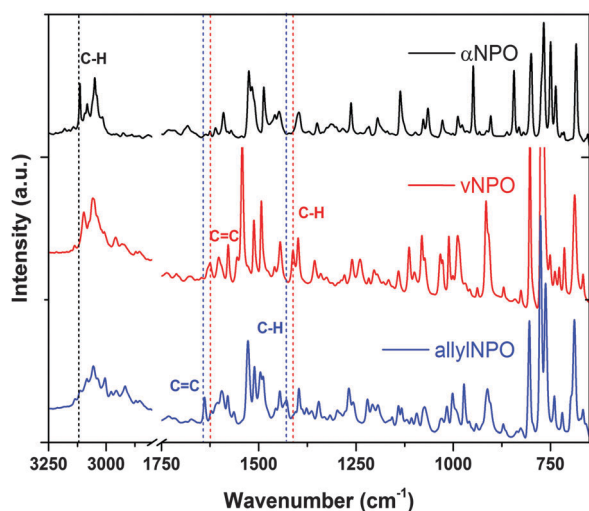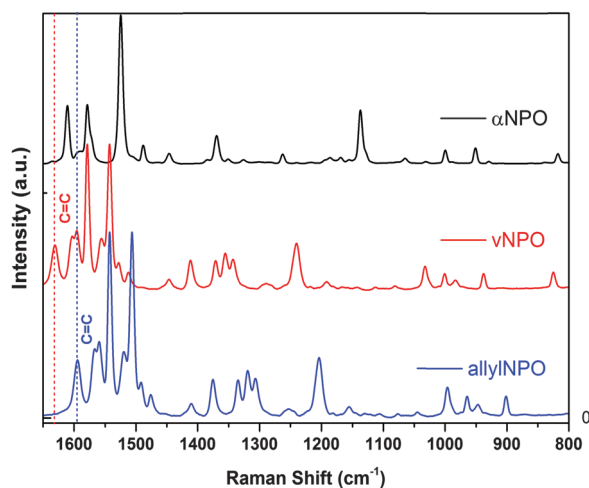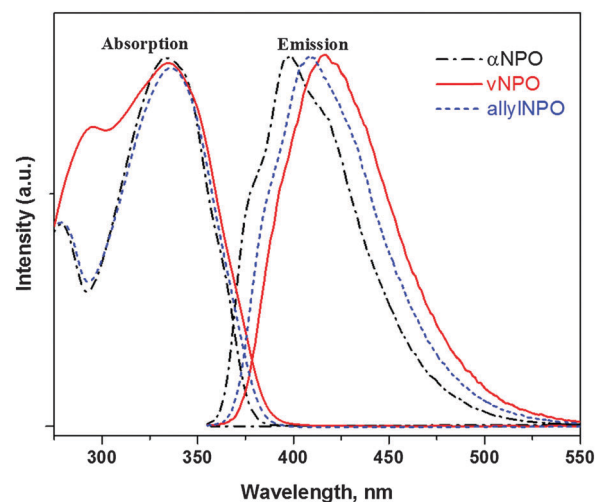

Fig. 4 Absorption and emission spectra of αNPO fluor, vNPO and allylNPO monomers in methyl acetate solutions.

7058 | J. Mater. Chem. C, 2015, 3, 7053–7061

This journal is © The Royal Society of Chemistry 2015

et al.[7] synthesized the monomer form of an organic scintillator 2-[4-(4′-vinylbiphenylyl)]-5-(4-*tert*-butylphenyl)-1,3,4-oxadiazole (vPBD). However, addition of an unbound wavelength shifter 1,4-bis[2-(2-methylphenyl)ethenyl]-benzene (bis-MSB) was essential to shift the radiative energy from vPBD at 370 nm to the violet range of 418 nm (Fig. S6, ESI†). Although the wavelength shifter solved the detection problem, no monomer form of this material or any other wavelength shifters are available, so the sensor performance will degrade from leaching out of the wavelength shifter during long term *in situ* monitoring applications. In this work, the absorption and emission data reveal that vNPO is an ideal organic fluor candidate for making stable extractive scintillating sensors, where it can be used alone without the need to add a wavelength shifter.

Table 1 reports the photophysical data of the monomers and their corresponding polymers. The date revealed a decrease in molar extinction coefficient of monomer forms relative to αNPO; however, this decline did not affect their scintillation efficiency. The fluorescence quantum yield (Φ_f) of vNPO and allylNPO relative to αNPO are similar and they lost only ~2.5% of Φ_f of the reference material which indicates that adding the unsaturated groups will not affect the scintillation properties of the new monomers. Fig. 5 presents the excitation/emission

spectra of the polymers. The graphs show that the vNPO and allylNPO retain their photophysical properties after covalent incorporation in the polymer matrix, maintaining nearly the same red spectral shift and order, which motivate further characterizations.

Scintillation properties and radiation detection

For the final application of aqueous monitoring of radioactivity, the scintillation properties of these materials must be evaluated with ionizing radiation. In the previous section, the fluorescence properties of the fluor monomers and their corresponding polymers were studied using UV energy. In this section the scintillation properties, the emission of visible light from the absorption of ionizing radiation, are quantified. A direct measurement of $^{99}TcO_4^-$ by a minicolumn sensor and static LSC was conducted after preconcentration using the scintillating resins functionalized with MDOA. The aim of this experiment was to evaluate the linearity and the optical performance of the new materials. Fig. 6 presents the background pulse height spectrum with counting rate of 0.56 ± 0.025 cps and the pulse height spectra corresponding to the P-vNPO and P-allylNPO resins after loading of 187 Bq of ^{99}Tc. Comparing the data reveals that P-vNPO sensor has a higher luminosity relative to the P-allylNPO sensor. This was determined by the shift in the P-vNPO pulse height spectrum to the right. Although the allylNPO resin has very little yellow color relative to vNPO, the decline of the peak height of P-allylNPO material is mainly attributed to the lower incorporation efficiency of allylNPO which found to be only 35% of the starting material (1.05% w/w), compared to >95% incorporation efficiency (2.85% w/w) for vNPO. Because of the higher incorporation efficiency of the vNPO scintillating anion-exchange sensor it was expected to have higher detection efficiency with all other variables being the same.

To evaluate the linearity responses of the P-vNPO and P-allylNPO scintillating sensors, two systems were tested by analyzing five

Table 1 Spectral parameters of compounds αNPO, vNPO and allylNPO, along with the corresponding polymers P-αNPO, P-vNPO and P-allylNPO

Sample	$\lambda_A{}^a$ (nm)	λ_F (nm)	ε^b (L mol^{-1} cm^{-1})	$\Phi_f{}^c$	$\Delta\nu^d$ (cm^{-1})
αNPO	333	402	18 309	1.00	5154
vNPO	338	425	11 445	0.97	6056
AllylNPO	337	418	13 415	0.98	5750
P-αNPO	377	405	—	—	1834
P-vNPO	391	419	—	—	1709
P-allylNPO	378	412	—	—	2183

^{a} λ_A and λ_E are maximum absorption and emission wavelengths for organic fluor and corresponding polymer. ^{b} ε is the molar extinction coefficient. ^{c} Φ_f is fluorescence quantum yield. ^{d} Stokes shift; $\Delta\nu = 1/\lambda_A - 1/\lambda_F$ in cm^{-1}.
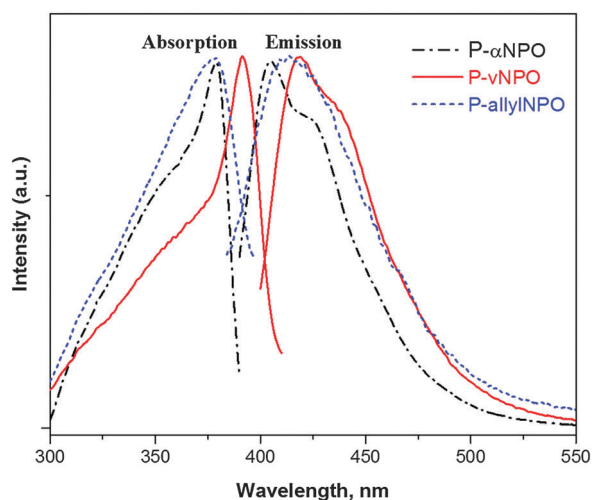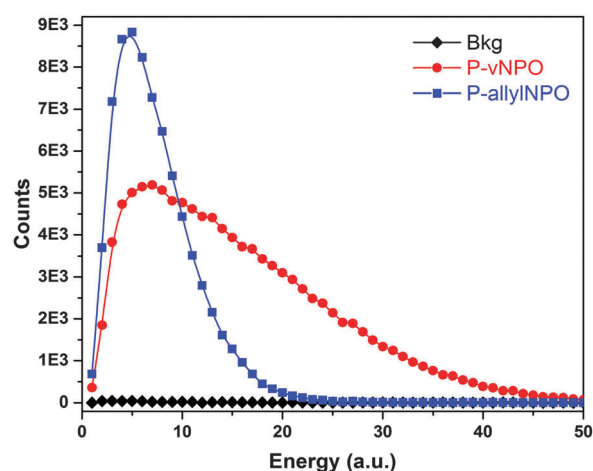

Fig. 5 Absorption and emission spectra of scintillating polymers P-αNPO, P-vNPO and P-allylNPO.

Fig. 6 Pulse height spectra collected for P-vNPO and P-allylNPO sensors after counting 187 Bq of $^{99}TcO_4^-$ for 15 minutes. The pertechnetate anion was loaded on MDOA quaternary ammonium group from 0.01 M HCl.
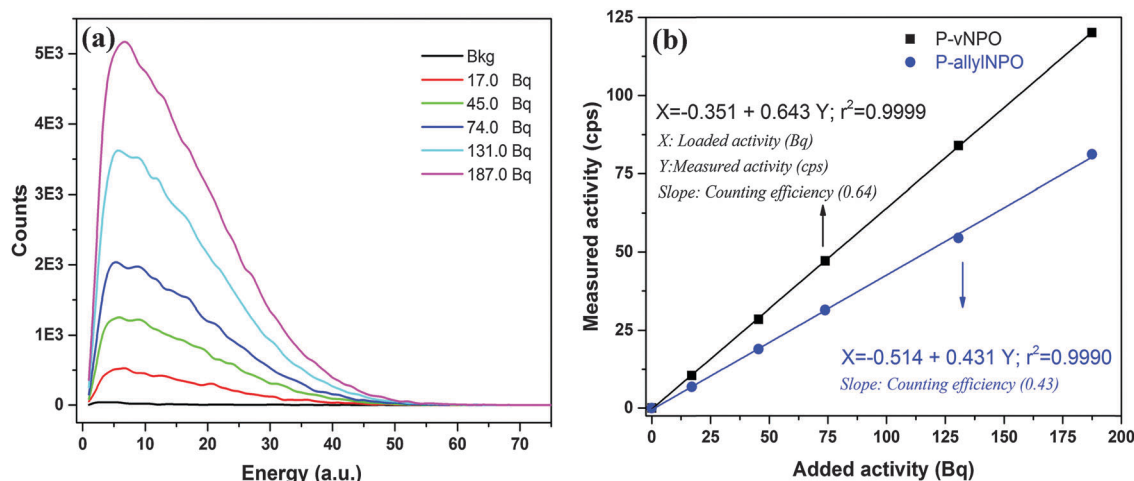
This journal is © The Royal Society of Chemistry 2015

J. Mater. Chem. C, 2015, **3**, 7053–7061 | 7059

Fig. 7 Quantification of ^{99}TcO$_4^-$ illustrating regular increasing peak areas with increasing standard activity (a) and the corresponding calibration curves for P-vNPO and P-allylNPO scintillating resins (b). The count time was 15 minutes for each standard; the uncertainty ranges of calibrations are 2.1–0.3% and 3.0–0.4% for P-vNPO and P-allylNPO.

standards of ^{99}Tc, covering the radioactivity range of 17–187 Bq (see Fig. 7). The corresponding scintillation spectra for the P-vNPO sensor after successive loading of five different activities of ^{99}Tc demonstrate good optical response as a function of increasing ^{99}TcO$_4^-$ concentration as represented in Fig. 7a. Both the P-vNPO and P-allylNPO sensors yielded linear calibrations with $r^2 > 0.999$ when the measured net spectrum areas were plotted against the loaded radioactivity levels of the ^{99}Tc standards. The net count rate, CR$_n$ in count per second (cps) can be related to sample activity, A_{Bq}, according to eqn (1):

$$CR_n = A_{Bq}E_dE_s \tag{1}$$

The parameters E_d (ratio of the counting rate detected to the decay rate in the sample) and E_s (the ratio of activity in the extracted ^{99}Tc to the injected sample activity) represent the detection and loading efficiencies of the analyte, respectively. The effective efficiency ($E_e = E_dE_s$) of the P-vNPO and P-allylNPO sensors can be determined directly from the slope of the calibration curves (Fig. 7b) to be 64.3% and 43.1%. The eluate after each loaded ^{99}Tc standard solution onto the column was collected and counted by conventional static LSC, and the results were summed to obtain the amount of ^{99}Tc activity that was not extracted by the scintillating anion exchange sensors. Since the ^{99}Tc activity in the injected sample was known, the E_s level was determined to be >99.5% for both materials. The average E_d values calculated for the five ^{99}Tc standards used were 63.2 ± 1.2% for the P-vNPO sensor and 41.8 ± 1.3% for the P-allylNPO sensor. This difference is mainly due to the final mass incorporated in the matrix which found to be 2.85% (w/w) and 1.05% (w/w) for vNPO and allylNPO, respectively. This conclusion can be further supported because both new monomers have similar quantum yields and the only clear difference is the incorporated mass. Both concentrations were used for the reported scintillation measurements. The final data demonstrate that we have succeeded in developing two stable scintillating resins that can be used to quantify radioactivity on an aqueous matrix.

However, only P-vNPO will be selected for further research due to its high organic synthesis yield, high incorporation efficiency and subsequent high counting efficiency. The material is ready for further characterization for the final application in environmental water quality monitoring and nuclear forensics.

Conclusions

In this work, two new monomers of 4-substituted 2-(1-naphthyl)-5-phenyloxazole (αNPO) were synthesized successfully with good chemical yield. The monomers include the vinyl and allyl forms of αNPO, which were copolymerized with 4-methylstyrene, divinylbenzene and 4-chloromethyl styrene to yield stable and transparent, spherical scintillating resin beads. The absorption and emission spectra show that vNPO has a strong absorption peak between 300 and 350 nm. The fluorescence data reveal that vNPO is an ideal organic fluor candidate for making stable extractive scintillating sensors, where it has emission of light in a spectral range detectable for photosensors such as a PMT with an average wavelength of ~420 nm. It can be used without the need for an additional wavelength shifter. To evaluate the energy transfer and subsequent scintillation process after energy deposition from the radiation particles, ^{99}Tc (as a pure beta emitter) was accumulated on the MDOA anion exchange groups attached to the scintillating beads. The results revealed that our P-vNPO functionalized scintillating resins possess high radiation detection efficiency (average of 64.5%). Thus, the prepared materials can be used for developing advanced extractive scintillating sensors with enhanced sensitivity and stability for natural waters quality monitoring and nuclear forensics.

Acknowledgements

7060 | J. Mater. Chem. C, 2015, 3, 7053–7061

This journal is © The Royal Society of Chemistry 2015

Notes and references

1 A. Thakkar, M. Fern, T. Kupka and J. Harvey, Application Note 009601-01, April, 2011, Gross Alpha Measurements in Aqueous Samples Using Extraction Chromatography and Liquid Scintillation Counting PerkinElmer, Inc., USA.

2 K. Kołacińska and M. Trojanowicz, *Talanta*, 2014, **125**, 131.

3 J. W. Grate, R. Strebin, J. Janata, O. B. Egorov and J. Ruzicka, *Anal. Chem.*, 1996, **68**, 333.

4 T. A. DeVol, O. B. Egorov, J. E. Roane, A. Paulenova and J. W. Grate, *J. Radioanal. Nucl. Chem.*, 2001, **249**, 181.

5 O. B. Egorov, S. K. Fiskum, M. J. O'Hara and J. W. Grate, *Anal. Chem.*, 1999, **71**, 5420.

6 A. F. Seliman, A. Samadi, S. M. Husson, E. H. Borai and T. A. DeVol, *Anal. Chem.*, 2011, **83**, 4759.

7 A. F. Seliman, K. Helariutta, S. J. Wiktorowicz, H. Tenhu and R. Harjula, *J. Environ. Radioact.*, 2013, **126**, 156.

8 M. Hamel, V. Simic and S. Normand, *React. Funct. Polym.*, 2008, **68**, 1671.

9 H. Bagán, A. Tarancón, L. Ye and J. F. García, *Anal. Chim. Acta*, 2014, **852**, 13.

10 A. N. Mabe, M. J. Urffer, D. Penumadu, G. K. Schweitzer and L. F. Miller, *Radiat. Meas.*, 2014, **66**, 5.

11 Y. Kobayashi, *Biological Applications of Liquid Scintillation Counting*, Elsevier Inc, London, Amesterdam, 2012.

12 N. Zaitseva, B. L. Rupert, I. Pawelczak, A. Glenn, H. P. Martinez, L. Carman, M. Faust, N. Cherepy and S. Payne, *Nucl. Instrum. Methods Phys. Res., Sect. A*, 2012, **668**, 88.

13 L. D. Hughes and T. A. DeVol, *Anal. Chem.*, 2006, **78**, 2254.

14 B. Clapham and A. Sutherland, *J. Org. Chem.*, 2001, **66**, 9033.

15 V. N. Bliznyuk, C. E. Duval, O. G. Apul, A. F. Seliman, S. M. Husson and T. A. DeVol, *Polymer*, 2015, **56**, 271.

16 M. A. Gauthier, I. Stangel, T. H. Ellis and X. X. Zhu, *Biomaterials*, 2005, **26**, 6440.

17 S. Chadha, W. H. Nelson, R. Emrich and E. Lindesmith, *Appl. Spectrosc.*, 1993, **47**, 475.

This journal is © The Royal Society of Chemistry 2015

J. Mater. Chem. C, 2015, **3**, 7053–7061 | **7061**